

Preparation and Characterization of Bamboo Fibers Coated with Urushiol-Ferric and Its Composite with Polypropylene

Hanyu Xue,¹ Qinhui Chen,^{1,2} Jinhua Lin¹

¹College of Chemistry and Material Science, Fujian Normal University, Fuzhou, Fujian 350007, China

²Fujian Key Laboratory of Polymer Materials, Fujian Normal University, Fuzhou 350007, China

Received 28 September 2009; accepted 12 September 2011

DOI 10.1002/app.35645

Published online 20 December 2011 in Wiley Online Library (wileyonlinelibrary.com).

ABSTRACT: To improve the interfacial adhesion of bamboo powder/plastic composites by using natural coupling agents, bamboo fibers (BFs) coated with urushiol-ferric (BCFeU) were obtained via *in situ* polymerization and BCFeU/polypropylene (PP) composites were prepared. Direct correlations were found between coating ratio of BCFeU and activation time, concentration of urushiol, reaction time and concentration of ferric chloride. Five methods consisting of polarizing microscope, scanning electron microscope, X-ray photoelectron spectroscopy, thermo gravimetric analysis, and differential scanning calorimetry were used to characterize the BCFeU. The results show that BCFeU was obtained successfully. Urushiol-ferric

compounds were coated on the BFs by hydrogen bonding. Tensile test results and scanning electron microscope analysis of tensile fracture surfaces showed that urushiol-ferric acted as a coupling agent in BCFeU/PP composite. This results in 56% increase in elongation at break and 46% increase in maximum deflection of BCFeU/PP composite (compared with that of BF/PP composite) while there was no evident of variation in tensile strength and bending strength. © 2011 Wiley Periodicals, Inc. *J Appl Polym Sci* 125: 439–447, 2012

Key words: biofibers; coatings; reinforcement; poly(propylene) (PP); composite

INTRODUCTION

Recently, the incorporation of cellulosic materials as a reinforcing component in polymer composites has received increasing attention, particularly for price driven and high volume applications.^{1–3} The potential advantages of bamboo fibers (BFs), apart from their environmental benefits, are the abundant availability of the raw materials from renewable resources and low cost, meanwhile, they have high specific strength due to their low density.^{4–6} However, the main drawback of BFs is its hydrophilic nature that results in incompatibility with hydrophobic polymeric matrices, which led to poor mechanical properties of composites.^{7–11}

Previous studies concerned with the improvement of interfacial adhesion of bamboo powder/plastic

composites (BPCs) were using petrochemicals additives (such as silane coupling agent and maleic anhydride).^{12–16} To the best of our knowledge, there is little literature to report the use of natural coupling agents to improve the interfacial adhesion of BPCs.

Chinese lacquer is the emulsion-like outflow of natural rhus. Urushiol is the main component of Chinese lacquer, which is a series of derivatives of pyrocatechol containing an unsaturated long side chain^{17,18} (Fig. 1). In this article, urushiol-ferric compounds were coated onto BFs via *in situ* polymerization. Since its weak polarity of hydroxyl on the benzene ring and compatibility of long carbon chain, urushiol-ferric compound is expected to play a role of compatibilizer in BPCs, which could improve the interfacial compatibility between hydrophilic BFs and hydrophobic plastic.

Correspondence to: J. Lin (jhl@fjnu.edu.cn).

Contract grant sponsor: Natural Science Foundation of Fujian Province; contract grant number: 2008J0227.

Contract grant sponsor: Project of Science and Technology Office of Fujian Province; contract grant number: 2007F5030.

Contract grant sponsor: Project of Fujian Education Department; contract grant number: JB10005.

Journal of Applied Polymer Science, Vol. 125, 439–447 (2012)
© 2011 Wiley Periodicals, Inc.

EXPERIMENTAL

Materials

BPs were purchased from local market, 80 mesh comminuted (the dimension of BPs was range from 5 to 15 μm and the aspect ratio was 10 : 1–20 : 1). Urushiol was purchased from Xi'an Lacquer Research Institute. It was extracted and 94 (wt %) urushiol was obtained. Isotactic polypropylene (PP)

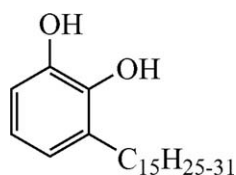


Figure 1 The chemical structure of urushiol.

homopolymer powder (PPH-XD-045, MFI = 2.1–6.0 g/10 min) was purchased from Shandong Kairi Chemical Industry Ltd. Co., China.

Preparation of BFs

The BFs are prepared as follow: 100 g of BPs were dispersed under vigorous stirring in 1000 mL of 9.5 wt % sodium hydroxide/4.5 wt % urea aqueous systems. The suspension liquid of BP was ultrasonic activated for 15 min (the frequency of ultrasonic was 40 KHZ). Then filtered and rinsed with 9.9 wt % sulfuric acid/10 wt % sodium sulfate mixed solution and 5 wt % sulfuric acid sequentially. Finally, the precipitation was filtered and rinsed with distilled water and dried at 100°C for 4 h.

Preparation of BCFeU

2.0 g of BFs were dispersed in 20.0 mL of ferric chloride aqueous solutions for 16 h (obtained BF-FeCl₃). After filtered, 20.0 mL of urushiol ethanol solution was added into BF-FeCl₃. After a period of reaction time, the product was filtered and rinsed with ethanol to remove the unreacted urushiol or ferric chloride. The final product (BFs coated with urushiol-ferric, BCFeU) was obtained after drying at 100°C for 2 h.

The weight gain rate (WPG %) of BCFeU relative to BF was calculated according to the following formula:

$$\text{WPG}\% = (W_{\text{BCFeU}} - W_{\text{BF}}) / W_{\text{BF}} \times 100\%$$

In the formula, the W_{BCFeU} is the weight of BCFeU and W_{BF} is the weight of BFs. The coating ratio of BCFeU was expressed at weight gain rate.

Preparation of BF/PP composite and BCFeU/PP composite

According to the directions listed on Table I, precalculated amount of PP with BF and BCFeU were premixed by a high-speed disintegrating machine (JFW-A, China, the mixing speed was 2600 r/min). Then, the mixtures were extruded by a twin screw extruder (Polylab Rheomix PTW24/28, Germany) at 170–190°C with a screw rotational rate of 50 r/min.

Finally, the extrusion materials were calendered into sheets (0.5 mm thick).

CHARACTERIZATION

Polarizing microscope

A Germanic Leica DM LP polarizing microscope was used to show the process of preparation of BCFeU. The magnification of polarizing microscope was 200.

Scanning electron microscopy

The micro-morphology of BP, BF, BF-FeCl₃, and BCFeU and tensile fracture samples of BF/PP composite, BCFeU/PP composite were examined using a JEOL 7500 scanning electron microscope (SEM), operated at 15 kV. Samples were mounted with conductive adhesive on copper stubs and then sputter coated with aurum.

X-ray photoelectron spectroscopy

For X-ray photoelectron spectroscopy (XPS) characterization, C1s, N1s, O1s, and Fe 2p core level spectra of BF and BF-FeCl₃ was recorded by an ESCALAB 250 X-ray photoelectron spectrometer with Mg K_α radiation (1253.6 eV).

Thermo gravimetric analysis

Thermo gravimetric analysis (TGA) was carried out using a METTLER TGA/SDTA851 under nitrogen atmosphere with a heating rate of 10°C/min. The temperature range was from 30 to 500°C. The weights of all specimens were ~ 3–5 mg.

Differential scanning calorimetry

Differential scanning calorimetry (DSC) testing was carried out on a METTLER DSC822^e differential scanning calorimeter under nitrogen atmosphere with a heating rate of 10°C/min. The temperature range was from 30 to 500°C. The weights of all specimens were ~ 3–5 mg.

TABLE I
Directions for BP/PP and BCFeU/PP Composites

	BF (g)	BCFeU (g)	PP (g)	Olefin (g)	Stearic Acid (g)
BF/PP	70	0	30	1	1
BCFeU/PP	0	70	30	1	1

Note: Olefin and stearic acid were used as lubricants.

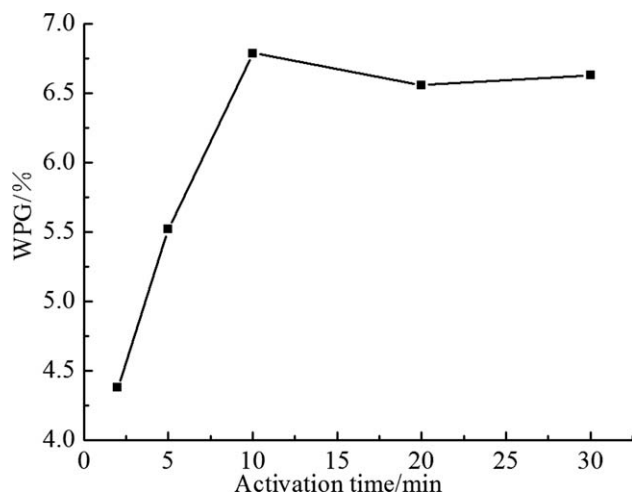


Figure 2 Effect of activation time on coating ratio of BCFeU (reaction conditions: concentration of urushiol, 10%; concentration of ferric chloride, 0.3 mol/L; reaction time, 30 min).

Mechanical properties

The tensile properties and bending properties of BCFeU/PP composites were tested on an universal testing machine, model LR5K (LLOYD, the United Kingdom), at a crosshead speed of 5 cm/min. Each value obtained represented the average of nine samples.

RESULTS AND DISCUSSION

Effect of activation time on coating ratio of BCFeU

There are special pores on the surfaces of hollow BFs which make it excellent in water absorbency and dyeing property. However, for bamboo powders (BPs), the hollow vascular bundles were blocked by oligosaccharides, ash, etc., which hindered the delivery of chemical reagents. Hence, pretreatment of BPs by ultrasonic activation is essential. Ultrasonic activation is one of the modern ways of chemical reactions accelerating and it also could be used for pretreatment of BPs. The major mechanism of the ultrasonic treatment of reagents is dispersion of sediments and flocculant particles by cavitation.¹⁹

Activation time played a dominant role in BPs' pretreatment as showed in Figure 2. With the prolonging of activation time, the coating ratio increased. It is obviously due to the fact that obstructions in hollow vascular bundles were transpired by cavitation of ultrasonic activation. It was the diffusion coefficient of ferric chloride which enlarged by the exclusion of vascular bundle obstruction that ultimately improved the weight gain rate of BCFeU. The effect of ultrasonic activation got max during activation time reached from 10 to 40 min so that little change on coating ratio was found for BCFeU.²⁰

Effect of concentration of urushiol on coating ratio of BCFeU

The coating ratio of BCFeU was found to be increased drastically by the addition of urushiol concentration (Fig. 3). This result indicated that the addition of urushiol concentration increased the amount of monomer. It is the increased monomer amount which increases the extent of reaction. However, the mutual entanglement of urushiol side chains led to the reduction of diffusion coefficient of urushiol, reflecting in the WPG% decreased slightly in the urushiol conc. % range of 10–90%.

Effect of concentration of ferric chloride on coating ratio of BCFeU

Figure 4 illustrated the effect of concentration of ferric chloride on coating ratio of BCFeU. It could be seen from the figure that coating ratio of BCFeU increased with the accretion of ferric chloride. The coating ratio displayed this behavior maybe depending on the concentration gradient between internal and external of vascular bundles. The concentration gradient enlarged the diffusion coefficient of ferric chloride, which led to the increase of adsorption amount of ferric chloride. It is the increased adsorption amount of ferric chloride that increased the coating ratio of BCFeU.

Effect of reaction time on coating ratio of BCFeU

The effect of reaction time on coating ratio of BCFeU is showed on Figure 5. The coating ratio of BCFeU progressively increased as the reaction time prolonged. This result was pronounced for the increase of reaction degree. Subsequently, the coating ratio of BCFeU decreased after the reaction time reached 40

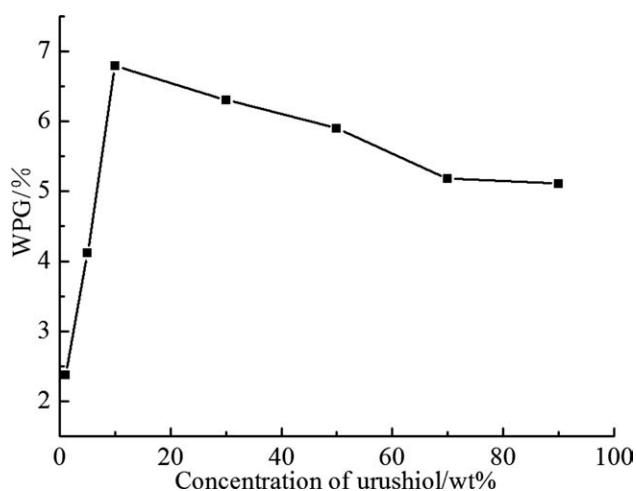


Figure 3 Effect of concentration of urushiol on coating ratio of BCFeU (reaction conditions: activation time, 15 min; concentration of ferric chloride, 0.3 mol/L; reaction time, 30 min).

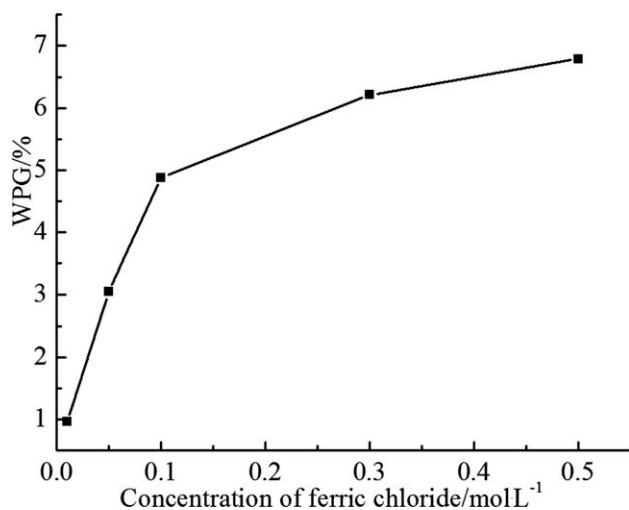


Figure 4 Effect of concentration of ferric chloride on coating ratio of BCFEU (reaction conditions: activation time, 15 min; concentration of Urushiol, 10%; Reaction time, 30 min).

min. This reduction was owing to the fact that the unreacted ferric ions diffused to the solution outside of vascular bundles of BFs.

Hence, the optimum preparation condition was obtained as follows: the activation time was 10 min; appropriate amount of BPs soaked in 0.5 mol/L ferric chloride aqueous solution then reacted with 10% urush-

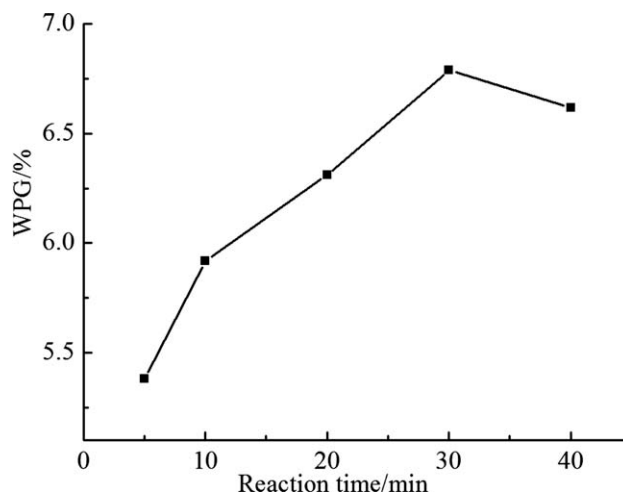


Figure 5 Effect of reaction time on coating ratio of BCFEU (reaction conditions: activation time, 15 min; concentration of urushiol, 10%; concentration of ferric chloride, 0.3 mol/L).

iol ethanol solution for 30 min. And BCFEU for processing was prepared under the optimum condition.

Polarizing microscope analysis

A polarizing microscope was used to show the process of preparation of BCFEU. It was observed from Figure 6(a) that vascular bundles of BPs were

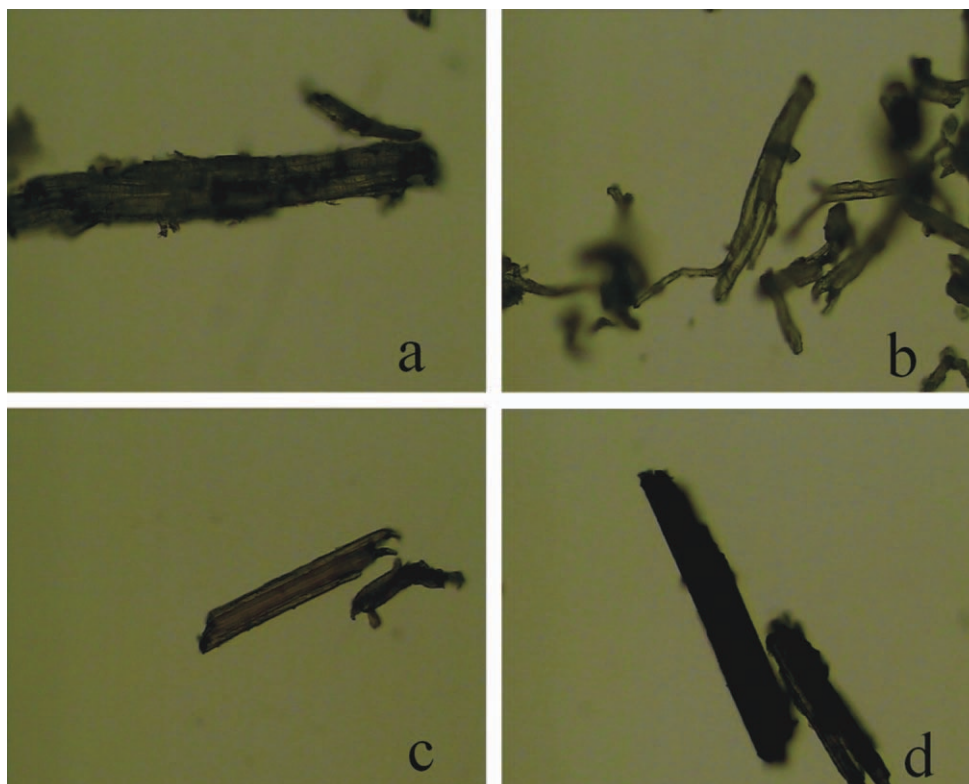


Figure 6 Polarizing microscope photomicrographs: BP (a), BF (b), BF-FeCl₃ (c), BCFEU (d) and the magnification of polarizing microscope was 200. [Color figure can be viewed in the online issue, which is available at wileyonlinelibrary.com.]

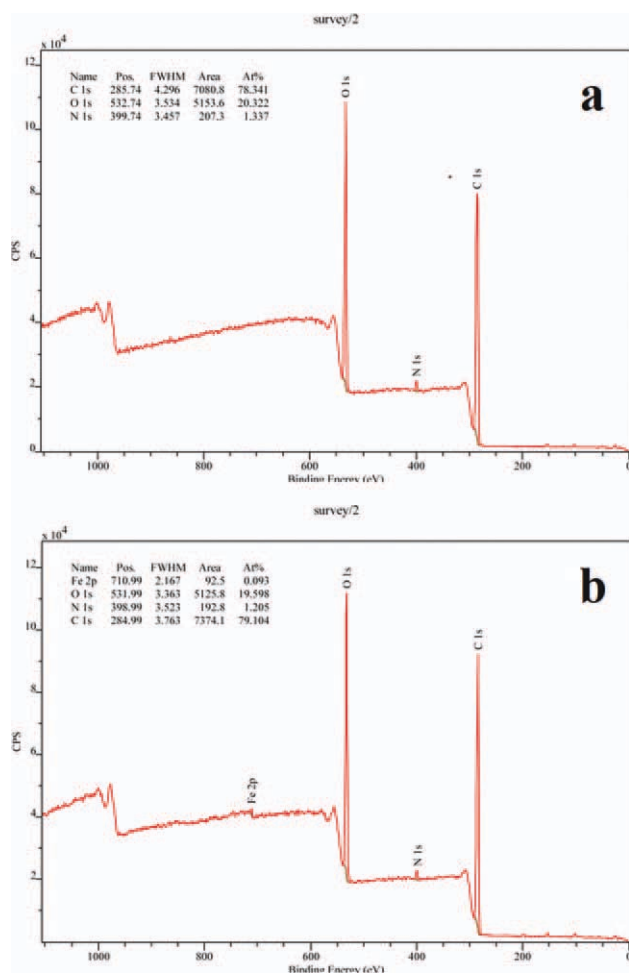


Figure 7 XPS spectra obtained for the surfaces [(a) BF, (b) BCFeU]. [Color figure can be viewed in the online issue, which is available at wileyonlinelibrary.com.]

blocked by oligosaccharides, ash, etc. After pretreatment, the obstructions in hollow vascular bundles were dissolved into lye transpired by ultrasonic activation [Fig. 6(b)]. Figure 6(c) shows that the vascular bundles of BPs presented henna after soaked in ferric chloride aqueous solution. This proves that the vascular bundles of BFs were filled with ferric chloride by capillarity. Finally, urushiol was added. *In situ* coordination reaction occurred between iron(III) and urushiol along the holes and vascular bundles. Hence, the appearance of BCFeU showed the characteristic black of urushiol-ferric complexes^{17,18} [Fig. 6(d)].

Surface chemical interaction analysis

To confirm the interaction between the hydroxyl groups on the surface of BFs and iron(III), the XPS surface analysis was used. The results of XPS surface analysis were showed on Figure 7. The Fe2p peak at 710.99 eV on X-ray pattern of BF-FeCl₃ [Fig. 7(b)] is not observed on X-ray pattern of BF [Fig. 7(a)]. The content of iron(III) was 0.093%. This low iron content can be explained by the low detection depth of XPS

TABLE II
Binding Energy Data from XPS of α - Ferric Oxide, Ferric Chloride, BF, and BF-FeCl₃

Compound	Binding energy (eV)	
	O1s	Fe2p
α - Ferric oxide	–	710.8
Ferric chloride	–	711.5
BF	532.74	–
BF-FeCl ₃	531.99	710.99

which are only a few nanometers, while most of iron (III) remain in the internal of BF vascular bundles.

XPS data listed in Table II showed the changes on binding energy of O1s and Fe2p. In water, ferric iron forms compounds that are often insoluble, at least near neutral pH. A salt of ferric iron hydrolyzes water and produces iron(III) oxide-hydroxides while contributing hydrogen ions to the solution. For BF-FeCl₃, the binding energy of Fe2p was lower than ferric chloride but significant close to that of α - ferric oxide.²¹ This suggested the formation of iron hydroxide gel during the hydrolysis of iron.^{21–23} Meanwhile, the binding energy of O1s for BF-FeCl₃ is 531.99 eV which is 0.75 eV lower than BF. The reduction of binding energy in O1s could be ascribed to that hydrogen bond interaction formed between hydroxyl groups on the surface of BP and iron hydroxide gel. Thus, the mechanism of iron hydroxide gel was adsorbed on BF could be inferred that the hydrolysis of iron(III) leads to the formation of iron hydroxide gel, then the iron hydroxide gel adsorbed onto the surface of BF by hydrogen-bonding (Fig. 8).

SEM analysis of BCFeU

An in depth analysis into microstructure of BCFeU was carried out by SEM. The results are shown in

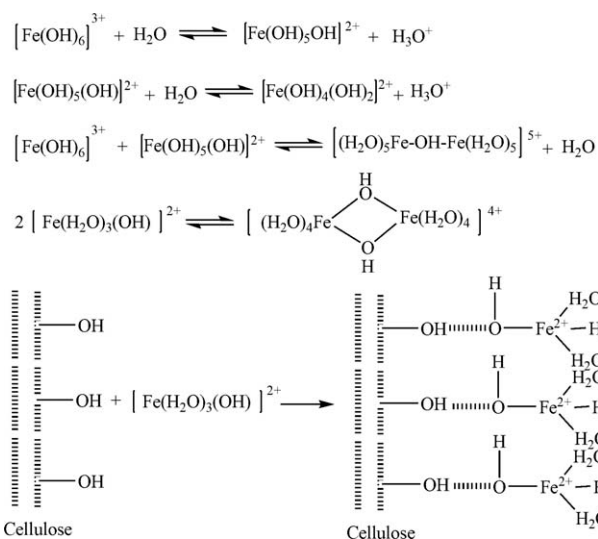


Figure 8 Mechanism of iron hydroxide gel adsorbed onto bamboo fiber.

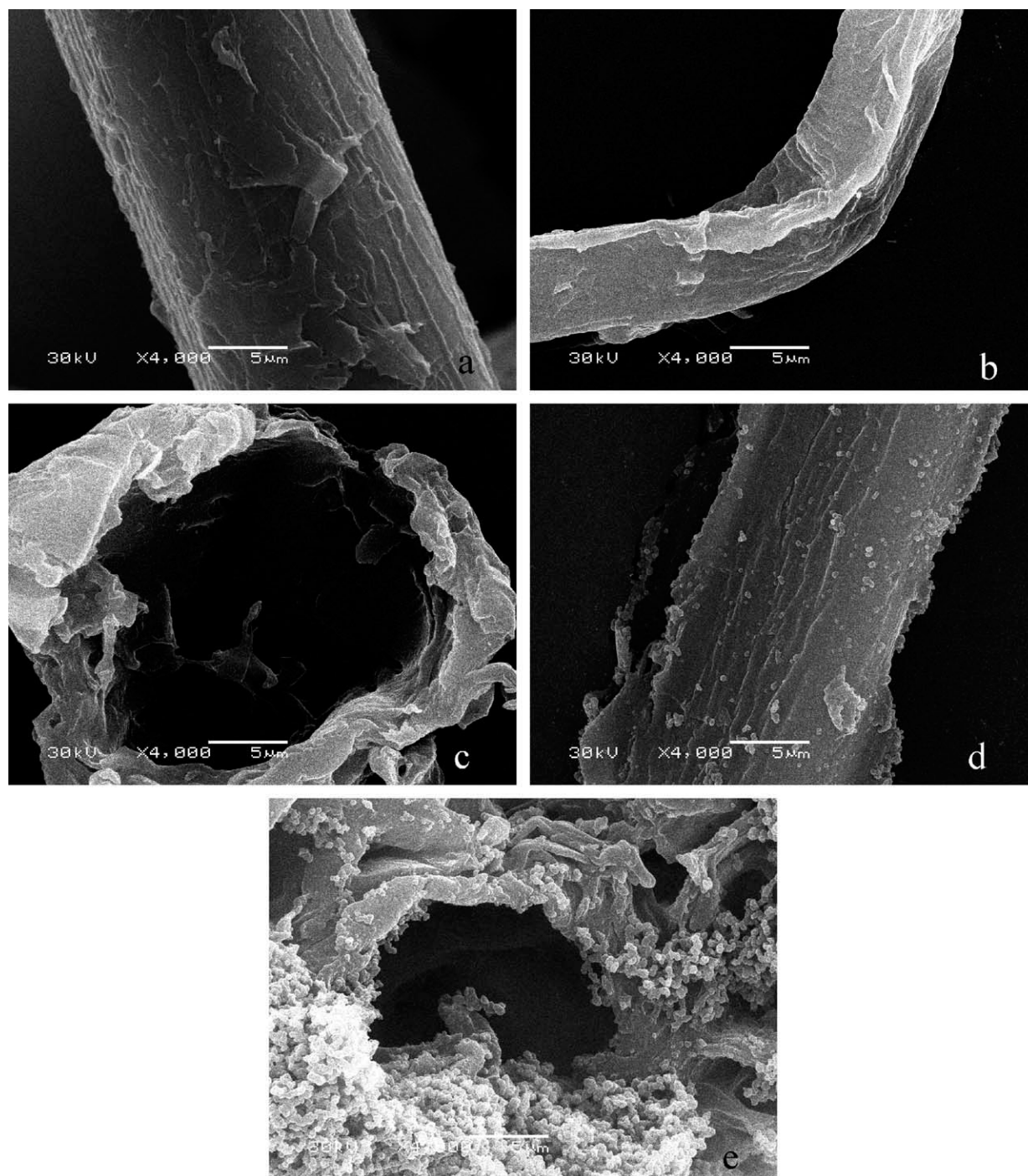


Figure 9 SEM photomicrographs of BP (a), surface of BF (b), Cross section of BF (c), surface of BCFeU (d), and cross section of BCFeU (e)

Figure 9(a–e). There are two basic types of vascular tissue, xylem and phloem [Fig. 9(a)]. The “phloem” part is formed by celluloses and hemicelluloses, while the lignins, the “xylem” part, assist and strengthen the attachment of hemicelluloses to celluloses, which present in the primary wall of the fibers.²⁴ After pretreatment, the “primary wall” was not observed from BF [Fig. 9(b)] and obstructions in hollow vascular bundles were transpired [Fig. 9(c)].

Figure 9(d,e) shows the surface and the cross section of BCFeU. We could get the conclusion from the comparison between Figures 9(b) and 3(d) that urushiol reacted with iron(III) Figure 10 along the holes on the surface of BP. Subsequently, urushiol-ferrous complexes polymerized (urushiol have an unsaturated side chain) under the catalysis of iron ions and heat. The granular polymers of poly-urushiol-ferrous coated onto the surface of BP [Fig. 9(d)]. It is

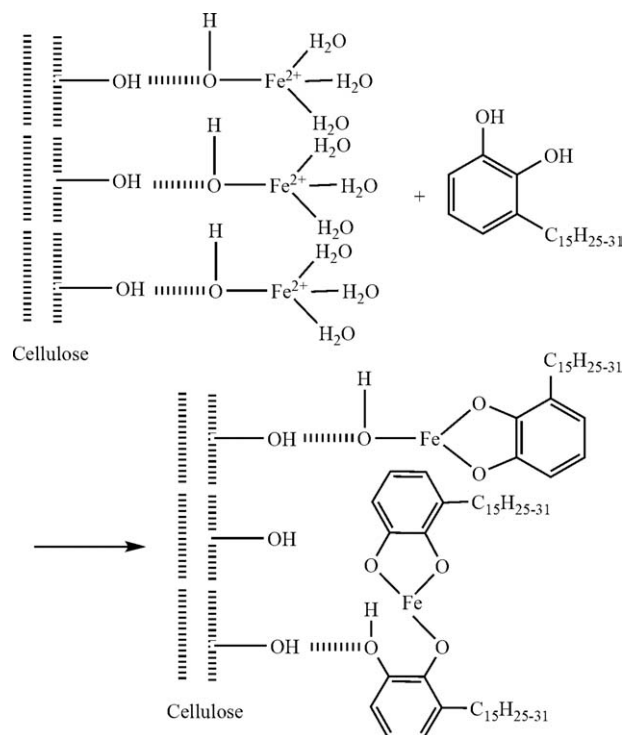


Figure 10 Mechanism of urushiol-ferric coated onto bamboo fiber.

the vascular bundles that the main reaction site for *in situ* polymerization, so more granular polymers were observed in the cross section of BCFeU [Fig. 9(e)].

Thermal decomposition process of BP and BCFeU

Thermal decompositions of BP and BCFeU were carried out by TGA and DSC analysis at a heating rate of 10°C/min. Typical TGA traces for BP and BCFeU are shown in Figure 11a. Three stages of decomposition were observed for both of them. Starting with dehydration and decomposition of volatile components at low temperatures (about 90°C), followed by rapid weight loss for thermal decomposition of hemicelluloses and lignin in an inert atmosphere (from 250 to 350°C), and finally decomposition corresponding to thermal decomposition of celluloses as the temperature increased. These stages also could be observed on DSC curves for BP and BCFeU [Fig. 11(b)]. For BP, there are two obvious endothermic peaks, one at 250°C which could be due to the thermal decomposition of hemicelluloses and the other at 370°C is the thermal decomposition of celluloses. However, it indicated that the endothermic peaks for BCFeU shifted to the lower temperature. The reason to explain this phenomenon maybe related to the crystallinity decreased after pretreatment as described previously.^{24,25} Meanwhile, this phenomenon could also be attributed to the polymerization of urushiol-ferric which released thermal energy (an

exothermic peak near 250°C on BCFeU DSC trace) accelerated the thermal decomposition.

Mechanical properties of composite

The pretreatment of BP removed not only the oligo-saccharides and ash in the vascular bundles but also the hemicelluloses and lignins. However, the hemicelluloses and lignins assist and strengthen the machine properties of celluloses.²⁵ Hence, although the pretreatment played an ideal role in the obstructions emptying, it reduces the machine properties of BFs.

In Figure 12, the basic tensile properties of the composites including tensile strength and elongation at break are depicted. It can be seen from the histograms that the elongation at break of BCFeU/PP composite reaches 56% which is higher than that of BF/PP composite, while no evident variation in tensile strength between the two composites is observed. The increase in elongation at break suggested that there was an enhanced adhesion between

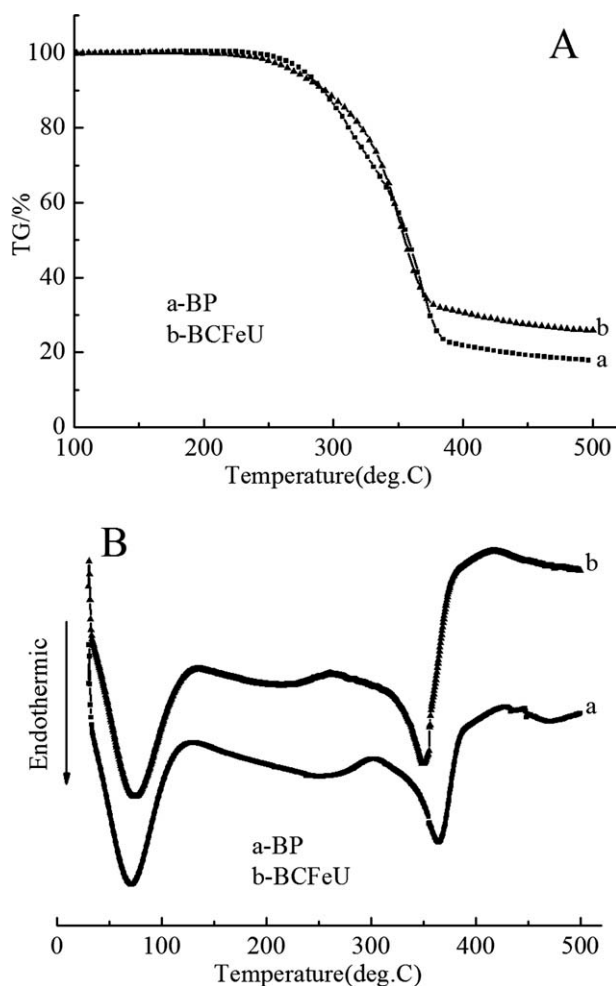


Figure 11 Thermal decomposition of BF and BCFeU were carried out by TG (a) and DSC (b) analysis at a heating rate of 10°C/min.

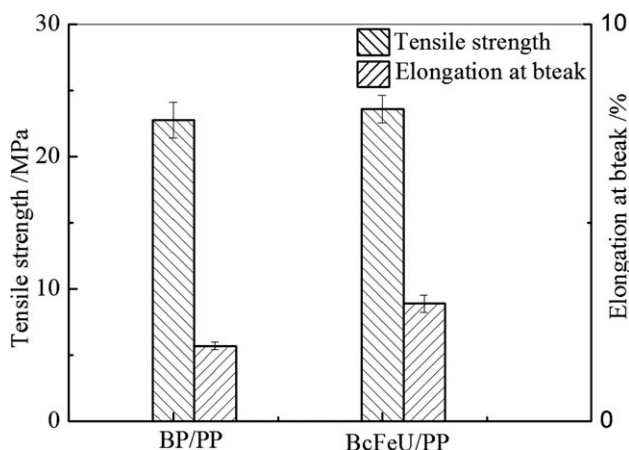


Figure 12 Tensile strength and elongation at break of BP/PP and BCFeU/PP.

BCFeU and PP matrix, which lead to a more efficient transfer of stress along the modified interface under loading.^{26–29} Therefore, it is the PP matrix that distorted to improved the elongation at break of BCFeU/PP composite. This result is verified by SEM analysis of BF/PP composite' fractured surface in the next section. The tensile strength which is supposed to be reduced did not changed also confirms this conclusion.

Table III shows the bending properties of composites. Comparable with BP/PP composite, the maximum deflection of BCFeU composite increases 46%. The increasing of maximum deflection suggests a synergistic behavior between PP matrix and BCFeU, which is able to divert the crack growth path and induce the formation of micro-cracking.^{28,29}

SEM analysis of BCFeU/PP composites

To elucidate the enhanced adhesion between BCFeU and PP matrix, the tensile fracture surfaces of composites were examined by SEM. Figure 13 shows the microphotographs of the tensile fracture surfaces of BP/PP composite and BCFeU/PP composite. A number of voids and unbroken BP were visible on the fractured surface of BP/PP composite [Fig. 13(a)] that could be due to the poor adhesion between BPs and PP matrix, which resulted in no effective reinforcement during tensile test. However, in Figure 13(b), obvious improvement was observed on the

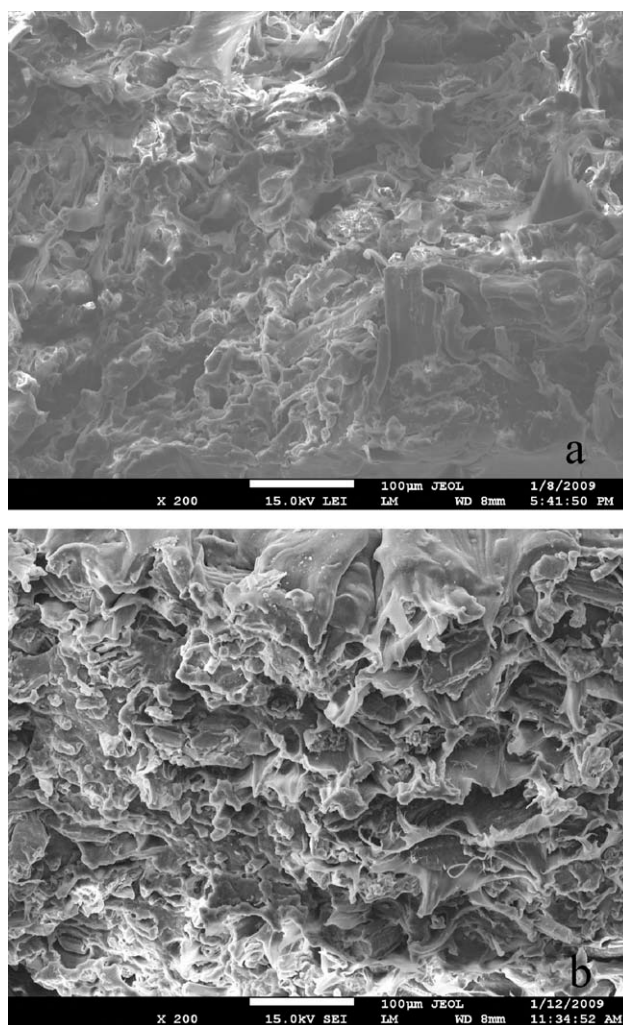


Figure 13 SEM photomicrographs of tensile fracture samples of BP/PP composite (a) and BCFeU/PP composite (b).

fractured surface of BCFeU/PP composite: extensive fibers fracture, less BPs pullout, and PP matrix deform significantly. A major reason for these improvements especially for the uniform stretched PP matrix could be that urushiol-ferric acted as a coupling agent in BCFeU/PP composite. As the BCFeU accounts for the vast majority of composite, applied tensile stress transferred from BFs to PP matrix through the improved interface bonding. Since PP matrix could distorted more effective, the elongation at break of BCFeU/PP composite improved.

CONCLUSION

A novel nature material BCFeU was obtained successfully by *in situ* polymerization. The *in situ* chemical reaction between urushiol and iron(III) supported on the surface of the BFs resulted in the formation of urushiol-ferric which coated on the surface of BFs by hydrogen-bonding. The urushiol-ferric

TABLE III
The Bending Properties of BP/PP and BCFeU/PP Composites

Samples	Bending strength (MPa)	Maximum deflection (mm)
BP/PP	40.6 ± 2.07	4.12 ± 0.42
BCFeU/PP	42.3 ± 2.85	6.04 ± 0.89

acted as a coupling agent in BCF_eU/PP composite, which result in 56% increase in elongation at break and 46% increase in maximum deflection of BCF_eU/PP composite when compared with that of BF/PP composite, while no evident variation in tensile strength and bending strength. Although the BCF_eU can not effectively improve the mechanical properties of BPCs, it still provide a new way (using of natural coupling agents) to improve the interfacial adhesion of BPCs.

REFERENCES

1. Beg, M. D. H.; Pickering, K. L. *Compos A* 2008, 39, 1091.
2. Beg, M. D. H.; Pickering, K. L. *Compos A* 2008, 39, 1565.
3. Alireza, A. *Bioresour Technol* 2008, 99, 4661.
4. Shinichi, S.; Yong, C.; Isao, F. *Compos A* 2008, 39, 640.
5. Navin Chand; Dwivedi, U. K. *J Mater Process Technol* 2007, 183, 155.
6. Mahuya, D.; Anindya, P. *J Appl Polym Sci* 2006, 100, 238.
7. Wong, K. J.; Zahi, S.; Low, K. O.; Lim, C. C. *Mater Des* 2010, 31, 4147.
8. Beg, M. D. H.; Pickering, K. L. *Polym Degrad Stab* 2008, 93, 1939.
9. Sanjay, K. N.; Smita, M.; Sushanta, K. S. *Mater Sci Eng A* 2009, 523, 32.
10. Hiroyuki, K.; Koichi, K.; Miki, F.; Hitoo, T.; Keisuke, K.; Kiyohiko I. *Compos B* 2009, 40, 607.
11. Yanjun, X.; Callum, A. S.; Zefang, X.; Holger, M.; Carsten, M. *Compos A* 2010, 41, 806.
12. Kazuya, O.; Toru, F.; Yuzo, Y. *Compos A* 2004, 35, 377.
13. Monini, S.; Gowri, V. S. *Polym Compos* 2003, 24, 428.
14. Xiaosong, H.; Anil, N. *Compos Sci Technol* 2009, 69, 1009.
15. Hiroyuki, K.; Koichi, K.; Miki, F.; Hitoo, T.; Keisuke, K.; Kiyohiko, I. D. *Compos B* 2009, 40, 607.
16. Kazuya, O.; Toru, F.; Erik, T. T. *Compos A* 2009, 40, 469.
17. Jinhua, L.; Binghuan, H. *Polym Mater Sci Eng* 1991, 5, 32.
18. Jianrong, X.; Yanlian, X.; Jinhua, L.; Binghuan, H. *Prog Org Coat* 2008, 61, 7.
19. Abramov, O. V.; Veksler, G. B.; Kulov, N. N. *Theor Found Chem Eng* 2009, 43, 568.
20. Fei, Y.; Qinglin, W.; Yong, L.; Weihong, G.; Yanjun, X. *Polym Degrad Stab* 2008, 93, 90.
21. Edward, L. K.; Mui, W.; Cheung, H.; Vinci, K. C. L.; Gordon, M. *Chem Res* 2008, 47, 5710.
22. Greenwood, N. N.; Earnshaw, A. *Chemistry of the Elements*, 2nd ed.; Butterworth, UK, 1997.
23. Burgess, J. *Metal Ions in Solution*; Horwood, 1978.
24. Bhardwaj, N. K.; Hoang, V.; Nguyen, K. L. *Bioresour Technol* 2007, 98, 1647.
25. Zhangying, C.; Wuhong, Y.; Qiuyi, P. *Bioresour Technol* 2010, 101, 7944.
26. Krzesin, M. S.; Zachariasz, J. J.; Ski, M.; Czajkowska, S. *Biore-sour Technol* 2008, 99, 5110.
27. Smith, F. W.; Hashemi, J. *Foundations of Materials Science and Engineering*, 4th ed.; McGraw-Hill, New York, 2006.
28. Hibbeler, R. C. *Statics and Mechanics of Materials*, SI Edition; Prentice-Hall, USA, 2004.
29. Mott, L. R. *Applied Strength of Materials*, 4th ed.; Prentice-Hall, USA, 2002.